9-20-2003

Perpendicular Transport Of Solar Energetic Particles In Heliospheric Magnetic Fields

Ming Zhang

Jack Randy Jokipii

Robert Bruce McKibben

THE ASTROPHYSICAL JOURNAL, 595:493–499, 2003 September 20

PERPENDICULAR TRANSPORT OF SOLAR ENERGETIC PARTICLES IN HELIOSPHERIC MAGNETIC FIELDS

MING ZHANG,[1] J. R. JOKIPII,[2] AND R. B. MCKIBBEN[3]
Received 2003 March 18; accepted 2003 June 3

ABSTRACT

This paper presents direct observational evidence for large perpendicular diffusive flows of solar energetic particles in heliospheric magnetic fields. Using anisotropy measurements of 40–92 MeV protons obtained by the High-Energy Telescope of the COSPIN consortium on *Ulysses* at high heliographic latitudes, we find that during several gradual solar particle events, for periods of many hours, the observed particle flow is directed at significant angles to the measured local magnetic field direction, which can only be explained by cross-field diffusion. The variation of the particle flow direction with the magnetic field direction seen in the 2000 July 14 solar energetic particle event has allowed us to derive a large $\kappa_\perp/\kappa_\parallel$ ratio of 0.25 with an error bar of less than 0.05. An upper limit of $\kappa_A/\kappa_\perp \leqslant 0.17$ is also found by analyzing the dependence of the particle anisotropy on the magnetic field polarity. The observation suggests that perpendicular diffusion of solar energetic particles cannot be neglected even in the early phase of a solar particle event.

Subject headings: diffusion — solar-terrestrial relations — Sun: magnetic fields — Sun: particle emission

1. INTRODUCTION

Diffusion and drift of energetic charged particles in turbulent magnetic fields are important processes that govern a variety of high-energy phenomena in astrophysical environments, such as the modulation of cosmic rays, interplanetary propagation of solar energetic particles, acceleration of charged particles by shock waves, and propagation of galactic cosmic rays in the interstellar medium. These processes in the heliosphere can be studied in great detail, because in situ measurements of magnetic fields and energetic particles can be made by many space-borne instruments, such as those on *Voyager*, *ACE*, and *Ulysses*, exploring various regions of the heliosphere. While our understanding of the diffusion in the direction parallel to the magnetic field is reasonably solid (Palmer 1982; Bieber et al. 1994), the perpendicular transport processes (both diffusion and drift) remain difficult to understand. There are many theories for the perpendicular transport (see, e.g., Jokipii 1966; Forman, Jokipii, & Owens 1974; Gleeson 1969; Forman & Gleeson 1975; Bieber & Matthaeus 1997; Giacalone & Jokipii 1994). The diffusion tensor may be written in terms of the parallel diffusion coefficient, $\kappa_\parallel$, the perpendicular diffusion coefficient, $\kappa_\perp$, and the antisymmetric diffusion coefficient, κ_A, as

$$\kappa_{ij} = \kappa_\perp \delta_{ij} + (\kappa_\parallel - \kappa_\perp) b_i b_j + \varepsilon_{ijk} b_k \kappa_A \ , \qquad (1)$$

where ε_{ijk} is the totally antisymmetric Levi-Civita epsilon. If the parallel mean free path $\lambda_\parallel$ is much greater than the gyroradius r_g, it can be shown that $\kappa_A = v r_g/3 = pcv/(3qB)$ (Isenberg & Jokipii 1979).

The value of $\kappa_\perp$ is poorly known. Over the years, many analyses have been done. The simple hard-sphere scattering result

$$\kappa_\perp = \frac{\kappa_\parallel}{1 + \Omega^2 \tau^2} , \qquad (2)$$

where Ω is the gyrofrequency and τ the characteristic timescale of particle scattering by turbulent magnetic fields, usually yields a very small ratio of $\kappa_\perp/\kappa_\parallel$, of the order of 10^{-5} or smaller, in the solar wind. However, it has been realized that this simple picture does not properly describe the perpendicular diffusion in the turbulent magnetic field. The field line random walk or mixing is missing, and it must be included. This has been included crudely using the quasilinear approximation (Jokipii 1966; Forman et al. 1974; Bieber & Mattheaus 1997). Numerical simulations carried out by Giacalone & Jokipii (1999) obtained $\kappa_\perp/\kappa_\parallel = 0.02$–$0.05$ for typical interplanetary conditions at 1 AU, a value much larger than the hard-sphere scattering result. Simulations of cosmic-ray transport in the heliosphere (Kota & Jokipii 1982) suggest that these higher values can explain cosmic-ray observations in the global heliosphere. However, there is as yet no completely satisfactory picture.

The experimental values of $\kappa_\perp/\kappa_\parallel$ derived from observations range from negligibly small to greater than 1. Model fits (see, e.g., Kota & Jokipii 1983; Reinecke, Moraal, & McDonald 1993, 1996) to the measurement of galactic cosmic-ray spectra require that the $\kappa_\perp/\kappa_\parallel$ ratio be less than 0.1, typically around 0.02. With the *Ulysses* high-latitude observations of the appearance of low-energy particles accelerated near the ecliptic by corotating interaction regions (CIRs), 27 day recurrent modulation of cosmic rays, and a very small latitude gradient of cosmic-ray fluxes, Jokipii & Kota (1995) suggested that the perpendicular diffusion coefficient in the latitudinal direction ($\kappa_{\perp\Theta}$) must be increased. More detailed models of cosmic-ray modulation (Potgieter 2000) suggested that the $\kappa_{\perp\Theta}/\kappa_\parallel$ ratio needs to be within the range 0.1–0.25. Fisk (1996) proposed a new model for the large-scale heliospheric magnetic fields that can connect the high-latitude region of the observations to a low-latitude

---

[1] Department of Physics and Space Science, Florida Institute of Technology, 150 West University Boulevard, Melbourne, FL 32901; mzhang@pss.fit.edu.

[2] Department of Physics, University of Arizona, 1118 East 4th Street, Tucson, AZ 85721.

[3] Department of Physics and Space Science Center, University of New Hampshire, Durham, NH 03824.

part of the heliosphere. In this picture, particles can move along the field lines to any latitude without the need of transport perpendicular to the magnetic field.

Dwyer et al. (1997) analyzed anisotropy measurements of low-energy (44–313 keV$/n$) helium associated with CIRs, and they derived very large values for the $\kappa_\perp/\kappa_\parallel$ ratios from 0.13 to 1.45. Intriligator & Siscoe (1995) also analyzed energetic ions associated with CIRs; however, they arrived at a considerably smaller $\kappa_\perp/\kappa_\parallel$ ratio.

A similar dilemma also exists regarding the transport of solar energetic particles. Before the demise of the solar flare myth in the early 1990s, solar flares were thought to be the source of solar energetic particles (SEPs). Because many energetic particle events were observed from Earth in association with solar flares that were not located on the west rim of the Sun, the particles were thought to have to rely on diffusion across coronal or interplanetary magnetic field lines (Reid 1964). With the discovery of the correlation between coronal mass ejections (CMEs) and large SEP events (Kahler, Hildner, & van Hollebeke 1978) and two classes of SEP events (Cane, McGuire, & von Rosenvinge 1986), Reames and colleagues (Reames 1999 and references therein) developed the current paradigm of particle acceleration of SEPs. The class of small, impulsive SEP events is produced by solar flares, which is basically the old paradigm of the particle acceleration, while the class of large, gradual SEP events is due to particle acceleration by CME-driven coronal and interplanetary shock waves. Because the CME shocks are much more extensive than the solar flares and they are not necessarily located around the flares, one does not have to have a direct magnetic connection to the flare site in order to see the particles. A dominant assumption for seeing SEPs is that the observer has to be connected to the acceleration site, either the flare or the CME shock front, by interplanetary magnetic field lines. This is because charged particle transport along the magnetic field lines has been thought to be much easier than cross-field transport. Zwickl & Roelof (1981) found that perpendicular transport of low-energy (~1 MeV) solar energetic particles is insignificant. Therefore, cross-field transport is neglected in most current models for the propagation of SEPs (Roelof 1969; Ng & Reames 1994). However, recent observations of SEPs by *Ulysses* (McKibben, Lopate, & Zhang 2001) found that essentially all the large solar energetic particle events can be seen from both *Ulysses* and Earth no matter how wide their latitude and longitude separations from the event on the Sun are, and that the flux levels at the two widely separate locations often become comparable within a few days after the event onset and remain so for the decay phase, lasting as much as a solar rotation. Such a phenomenon was sometimes called the reservoir effect of SEP events. It suggests that the transport of SEPs perpendicular to the average Parker interplanetary magnetic fields should be important too. But controversy still remains as to whether it is due to cross-field transport or excursion of the magnetic field line from the ideal Parker spirals.

This paper presents an analysis of the anisotropy measurements of 40–90 MeV protons from the 2000 July 14 (day 196) SEP event. The analysis provides compelling evidence for a large perpendicular diffusion flow at *Ulysses* in the early phase of the event. A ratio of $\kappa_\perp/\kappa_\parallel$ is derived for this event. A limit also is placed on the value of the $\kappa_A/\kappa_\perp$ ratio. Similar evidence for perpendicular transport in a few other SEP events is also shown.

2. OBSERVATIONS

We use anisotropy measurements of energetic particles from the High-Energy Telescope (HET) of the Cosmic and Solar Particle Investigation (COSPIN) consortium on *Ulysses*. The HET is mounted with its aperture perpendicular to the spin axis of the *Ulysses* spacecraft, which spins at ~12 rpm. Anisotropy measurements for energetic protons are made in the energy range of 40–92 MeV (H45 sectored counting rate). For details of the instrument, see Simpson et al. (1992). Figure 1 shows the geometry of the sector measurement of the HET on day 196 of 2000. At that time, *Ulysses* was at 3.17 AU radial distance from the Sun and S62° heliographic latitude. An X-5 solar flare occurred on the Sun at N22° latitude approximately on the opposite side of the *Ulysses* longitude (Zhang et al. 2003). A very fast halo CME associated with the flare was observed from Earth heading in that direction. An analysis of the time profile of the solar energetic particle event has been presented in Zhang et al. (2003).

We have fitted eight-sector H45 hourly average counting rates with a sum of harmonics up to the second order (see Fig. 2 caption). Figure 2 shows the obtained fitting parameters for the SEP event on day 196 of 2000. The direction of particle flow (first-order anisotropy direction) is shown in the HET scan plane, together with the magnetic field direction measured by the magnetometer experiment on *Ulysses* (Balogh et al. 1992). Substantial first-order anisotropy appears as soon as the counting rate exceeds the statistical threshold for meaningful determination of anisotropy, and its magnitude diminishes very gradually. The anisotropy is measured in the spacecraft reference frame; thus, it should contain the Compton-Getting effect. The magnitude of

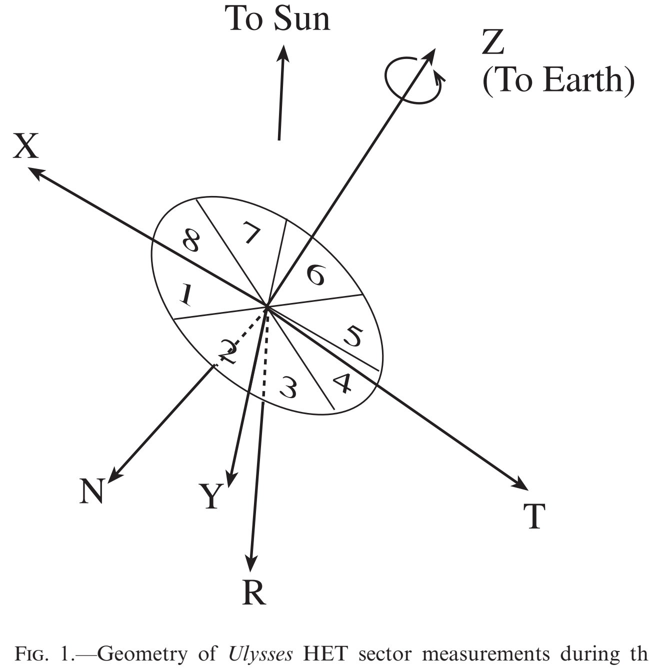

FIG. 1.—Geometry of *Ulysses* HET sector measurements during the 2000 July 14 event. X, Y, and Z are despun spacecraft coordinates, which are defined by the Z-axis pointing toward the Earth and the X-axis pointing to the projection of the Sun onto the plane normal to the spin axis. Reference to the normal RTN heliospheric coordinates is also shown. The anti-Sun direction, R, is in the X-Z plane and about 20° to the spin axis. The N- and T-axes are within 20° of the scan plane of the HET, while the T-axis is mostly in the $-X$ direction and N mostly in the Y direction.

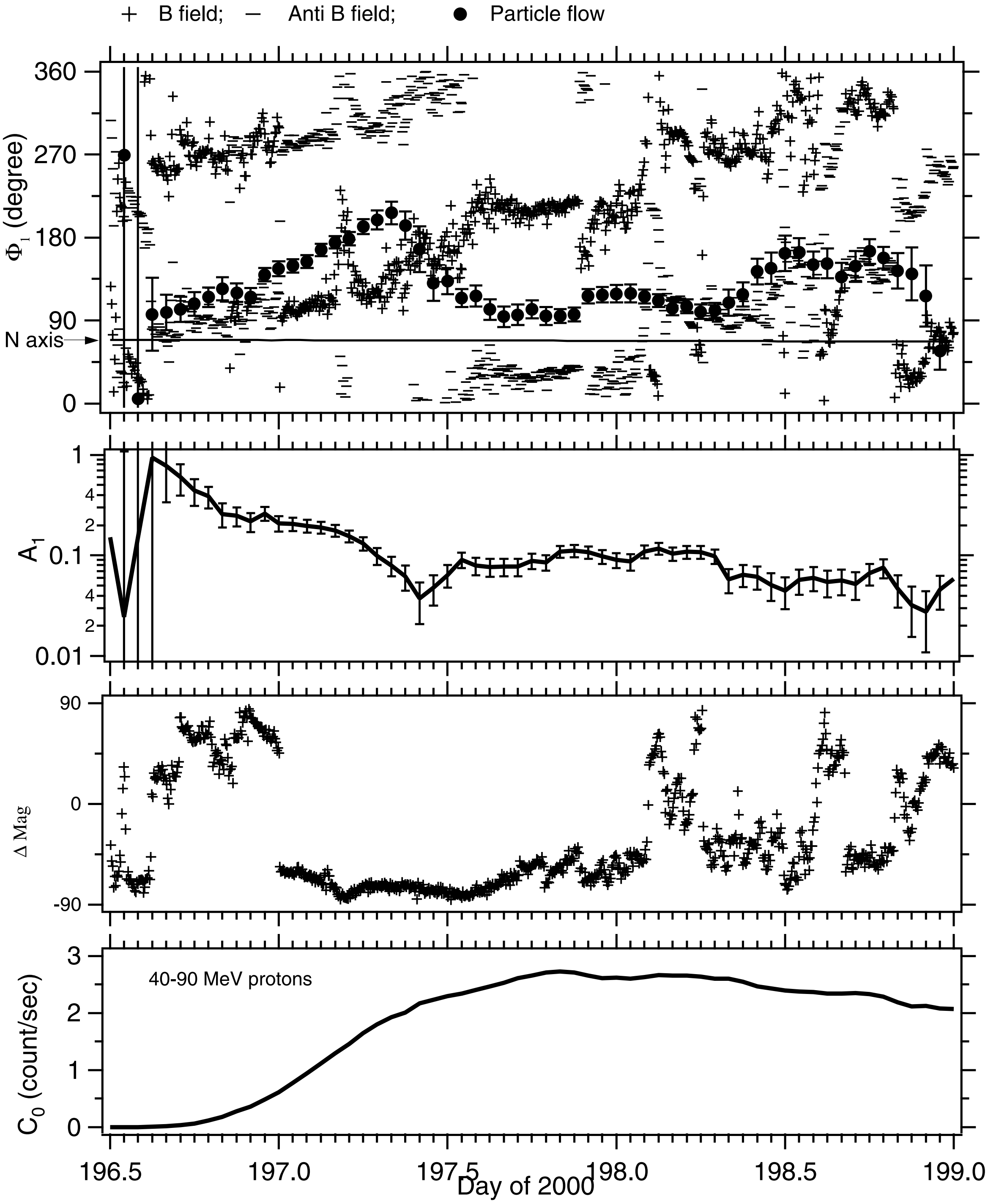

FIG. 2.—Fitting parameters to the *Ulysses* HET sector H45 hourly average counting rates for 40–92 MeV protons. The fitting function is a sum of harmonics up to the second order, i.e., $C_0[1 + A_1\cos(\varphi - \Phi_1) + A_2\cos(2\varphi - 2\Phi_2)]$, where C_0 is the spin average counting rate (*bottom*), A_1 and A_2 are the amplitude of first- and second-order anisotropies, and Φ_1 and Φ_2 are the azimuth angles of the anisotropies to the X-axis of the spacecraft despun coordinate system. For comparison with the anisotropy direction (*circles with error bars*), the projection of the (5 minute average) magnetic field direction on to the plane vertical to the spin axis of the spacecraft is shown by both the plus symbol for $\boldsymbol{B}$ and the minus symbol for $-\boldsymbol{B}$. The horizontal lines in the Φ_1 panel indicate the direction pointing toward the low latitude; Δmag is the elevation angle of magnetic fields to the scan plane of *Ulysses* HET. The second-order anisotropy does not affect the determination of the first-order anisotropy and thus is not shown here.

Compton-Getting anisotropy by convection with the solar wind is $A_{1,\mathrm{sw}} = 2(\gamma + 1)V_{\mathrm{sw}}/\nu$, where V_{sw}/ν is the ratio of solar wind speed to the particle speed and γ is the index of the power-law spectrum of the particles. At that time, the *Ulysses* solar wind plasma experiment measured a solar wind speed of ~650 km s^{-1}. At the energy of the H45 sector channel, the expected maximum anisotropy from the Compton-Getting effect is about 4% for the observed power-law spectrum, with a slope of about 2 for the entire event if the solar wind speed lies in the scan plane of the telescope. In fact, because the solar wind is almost perpendicular to the scan plane (see Fig. 1) and the spectral index is less than 2 in the early phase of the event, we expect a much smaller Compton-Getting effect. The magnitude of the first-order anisotropy shown in Figure 2 is over 10% for most of the time period, and in the early phase it is over 50%. This indicates that the first-order anisotropy appearing in this event cannot come from the Compton-Getting effect. Therefore, we do not have to make a correction for the Compton-Getting effect, as was done by Dwyer et al. (1997) for particles of much lower energies. Then the particle anisotropy shown in Figure 2 can be considered to represent the true particle flow relative to the magnetic field of the solar wind.

The azimuth angle of the first-order anisotropy (Φ_1), for most of the time during the phase of increasing flux, is not along the magnetic field direction projected onto the scan plane. At first, it tries to follow the changing magnetic field direction, while the difference gets bigger and bigger. Once the azimuth angle of the magnetic field reaches a certain value, the anisotropy direction swings in the opposite way. In the time period 1200–2400 UT on day 197, the first-order anisotropy becomes almost perpendicular to the projected magnetic field direction. This behavior indicates that the first-order anisotropy cannot entirely come from particle streaming along the magnetic field lines. In fact, because the magnetic field is almost perpendicular to the scan plane of the telescope (see the Δmag panel in Fig. 2), we expect a smaller anisotropy even if there is significant streaming along the magnetic fields. Therefore, there must be a particle transport perpendicular to the local magnetic field.

The anisotropy perpendicular to the local magnetic field may come from two sources, both related to the diffusion tensor and particle density gradient. One is drift anisotropy:

$$\boldsymbol{A}_{1,\mathrm{drift}} = \frac{3\kappa_A}{v}\hat{\boldsymbol{b}}\times\nabla\ln f \ , \tag{3}$$

where $\hat{\boldsymbol{b}}$ is the unit vector of the magnetic field direction and the gradient vector of particle density. The other is diffusion anisotropy:

$$\boldsymbol{A}_{1,\mathrm{diff}} = \frac{3}{v}\kappa_S\cdot\nabla\ln f \ , \tag{4}$$

where κ_{7S} is the symmetric part of the diffusion tensor in equation (1). Notice that the direction of the first-order anisotropy does not change when the magnetic field switches its polarity around 0000 UT on day 197. This clearly rules out the contribution from the drift anisotropy since the gradient of particle density is not expected to switch to the opposite direction at exactly the same time. Therefore, we conclude that there must be a large cross-field diffusion flow that can produce the observed cross-field first-order anisotropy.

3. ANALYSIS

Given that the particle first-order anisotropy comes entirely from the diffusion flow, we can derive from equation (4) the vector components of the anisotropy in the scan plane of the telescope:

$$\begin{aligned} A_{1x} &= \frac{\lambda_\parallel}{L}\left[\left(1-\frac{\kappa_\perp}{\kappa_\parallel}\right)\sin\theta_m\cos\varphi_m\hat{\boldsymbol{b}}\cdot\hat{\boldsymbol{g}}+\frac{\kappa_\perp}{\kappa_\parallel}\sin\theta_g\cos\varphi_g\right] \ , \\ A_{1y} &= \frac{\lambda_\parallel}{L}\left[\left(1-\frac{\kappa_\perp}{\kappa_\parallel}\right)\sin\theta_m\sin\varphi_m\hat{\boldsymbol{b}}\cdot\hat{\boldsymbol{g}}+\frac{\kappa_\perp}{\kappa_\parallel}\sin\theta_g\sin\varphi_g\right] \ , \end{aligned} \tag{5}$$

with

$$\hat{\boldsymbol{b}}\cdot\hat{\boldsymbol{g}} = \sin\theta_m\sin\theta_g\cos(\varphi_m-\varphi_g)+\cos\theta_m\cos\theta_g \ , \tag{6}$$

where $L = |\nabla\ln f|^{-1}$ is the scale size of the particle density gradient and the angles θ_m, φ_m, θ_g, and φ_g (θ is the angle from the spin axis Z and the angle in the scan X-Y plane) define the direction of the magnetic field, $\hat{\boldsymbol{b}}$, and the particle gradient, $\hat{\boldsymbol{g}}$, respectively. Then the azimuth angle of the first-order anisotropy (φ_1) is simply

$$\tan\varphi_1 = \frac{A_{1y}}{A_{1x}} \ . \tag{7}$$

If we assume that on the timescale of hours, over which the magnetic field direction changes rapidly, other quantities in equation (5), such as the particle density gradient and diffusion coefficients, remain constant, then we can determine the anisotropy from the magnetic field direction with these assumed constant parameters.

In Figure 3 the heavy curves are the results of calculation from equations (5) and (7). For comparison, the azimuth angle of the first-order anisotropy expected for particle streaming along or against the magnetic field lines is shown by the light curve. Obviously, the field-aligned streaming cannot explain the deviation of the anisotropy from the magnetic field direction, not even roughly the behavior in the variation of the azimuth angle. On the other hand, with the assumed parameters of the particle gradient and diffusion coefficients as listed in Table 1, we are able to match the observed variation of the azimuth angle of the anisotropy to the diffusion calculation very well. We choose only to match the later part of the event, because there the anisotropy direction is almost perpendicular to the magnetic field direction and the anisotropy should almost be entirely due to perpendicular diffusion. The good match of the diffusion calculation to the observation can also be noticeably seen in the anisotropy amplitude in the feature around 1100 UT on day 197, when the direction of diffusion flow becomes roughly perpendicular to the scan plane of the telescope and the azimuth anisotropy reaches a minimum. The diffusion calculation cannot fit the observation for the entire period, particularly in the early part of the event. This is expected because there is a stronger effect of particle streaming and the diffusion approximation may be less valid. Another problem early in the event is that gradients are probably changing rapidly, thus violating one of the assumptions of the model. The observed anisotropy direction falls in between the diffusion calculation and the streaming calculation, indicating that both effects are there even in the very early part of the event. Of course, some discrepancy exists in the anisotropy amplitude, probably because our assumption of a fixed $\lambda_\parallel/L$ ratio is too simple-minded. We have also

TABLE 1

VALUE OF THE PARAMETERS USED IN THE CALCULATION OF DIFFUSION ANISOTROPY

Parameter	Value
$\lambda_\parallel/L$	1.00
$\kappa_\perp/\kappa_\parallel$	0.25
θ_g (deg)	37
φ_g (deg)	160

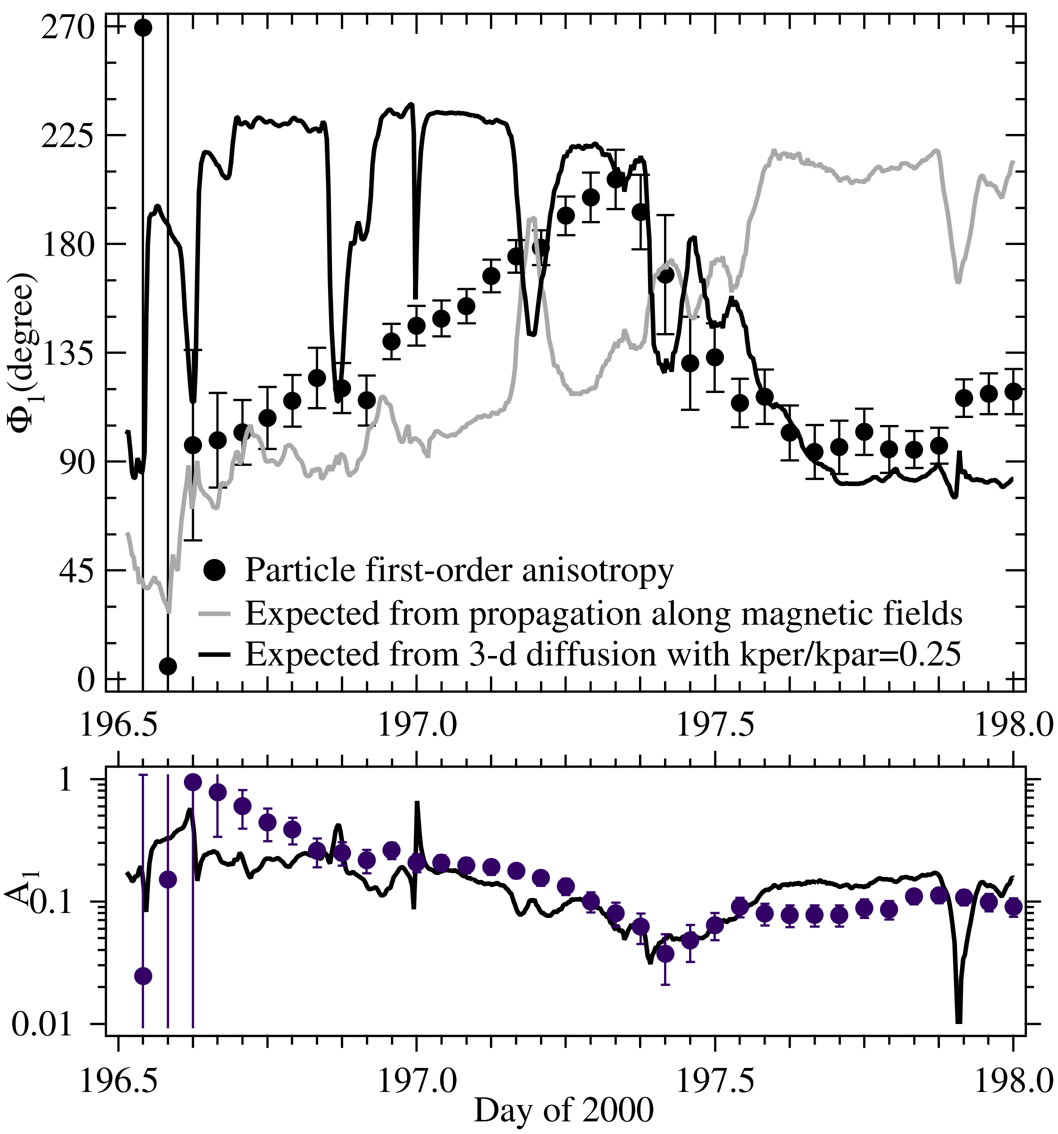

FIG. 3.—Azimuth angle (φ_1) and the amplitude (A_1) of the first-order anisotropy with their model expectation based on three-dimensional diffusion flow (*heavy curve*) and particle streaming along or against magnetic field lines (*light curve*).

tried to fit the anisotropy with the drift anisotropy (eq. [3]), but we cannot find any parameters for a fixed particle gradient that can produce a good match to the feature we see in the variation of the anisotropy around 1100 UT on day 197.

The calculation of the diffusion anisotropy is very sensitive to the parameters we choose in Table 1. We found that a roughly ±20% deviation in the $\kappa_\perp/\kappa_\parallel$ ratio, ±5° in θ_g, or ±20° in φ_g can result in dramatic changes in the calculation results of the anisotropy direction. We do not try to do a best fit to the data because we cannot completely separate out the effects of particle streaming. In addition, the calculated anisotropy is a function of both θ_m and φ_m; a fit to a two-dimensional function cannot easily be demonstrated by a curve.

The observed significant cross-field anisotropy requires a high value for the $\kappa_\perp/\kappa_\parallel$ ratio. This is a robust result from the observation because any $\kappa_\perp/\kappa_\parallel$ ratio much smaller than 0.1 would make the second term in A_{1x} and A_{1y} in equation (5) negligible and the anisotropy always along the magnetic field direction. A similar high value for the $\kappa_\perp/\kappa_\parallel$ ratio is also found in low-energy particles accelerated by CIRs (Dwyer et al. 1997).

Modeling of the time profile of particle intensity with the focused transport equation found that the parallel mean free path is around 0.07 AU for this event at *Ulysses* (Zhang et al. 2003). This mean free path corresponds to a parallel diffusion coefficient ($\kappa_\parallel$) of 3×10^{21} cm^2 s^{-1} for 50 MeV protons. Then the perpendicular diffusion coefficient ($\kappa_\perp$) is 8×10^{20} cm^2 s^{-1}. Diffusion coefficients similar to these magnitudes are often used in the modeling of cosmic-ray modulation and solar energetic particles propagation, but a $\kappa_\perp/\kappa_\parallel = 0.25$ ratio is new.

Translated to the RTN coordinates, the direction of the gradient shown in Table 1 is ~130° from the radial direction and ~70° from north, which is roughly consistent with particles coming from the Sun and low latitudes. The gradient component in the T-axis direction (from the west) is actually larger than the north component, indicating that stronger particle flow is coming from the west than from the north.

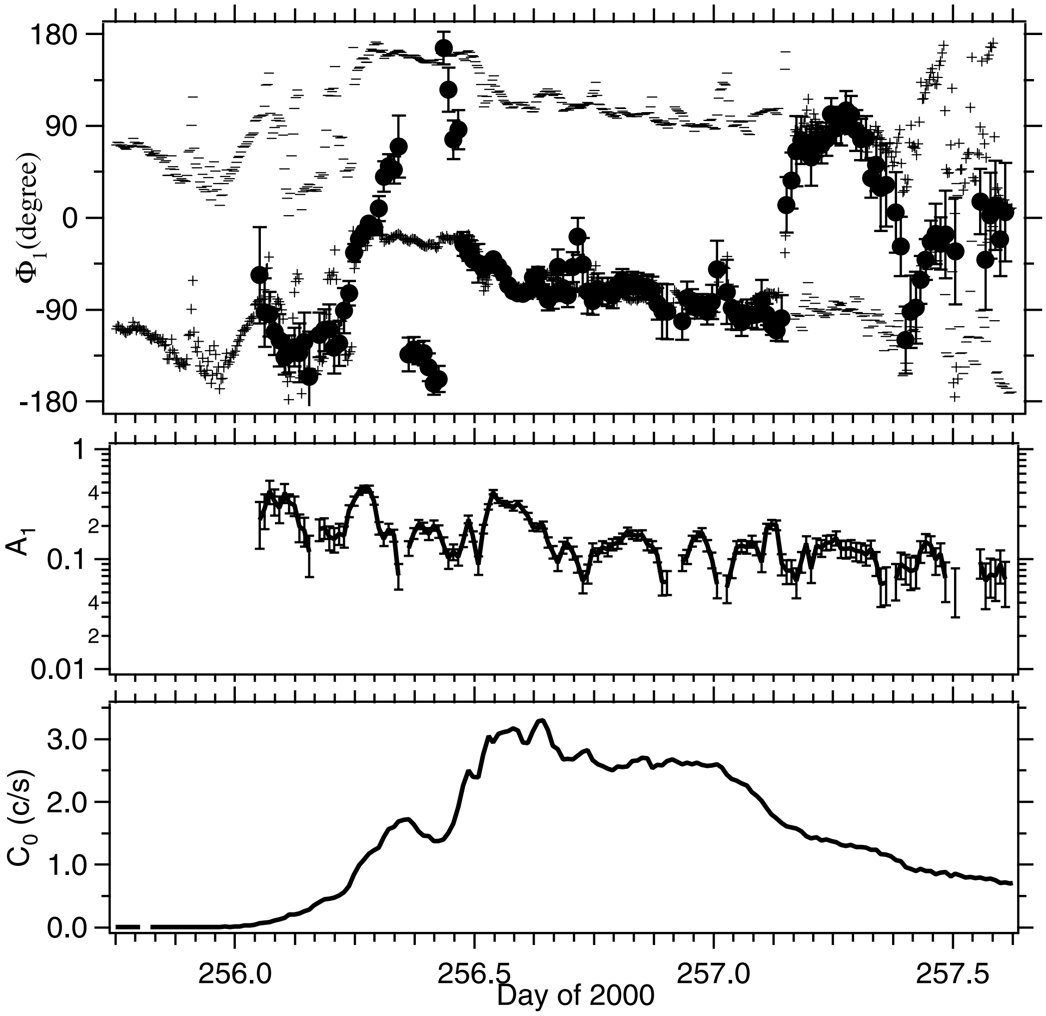

FIG. 4.—The 15 minute averages of anisotropy parameters for the 2000 September 14 event. See Fig. 2 for the format.

The scale size of the particle density gradient (L) needs to be comparable to the parallel mean free path (0.07 AU for $\sim$100 MeV protons) in order to produce the magnitude of the first-order anisotropy we observe here. Such a large particle density gradient cannot spread over the entire inner heliosphere; otherwise, particle density at 1 AU would be 12 orders of magnitude higher than at *Ulysses*. Large perpendicular diffusion flow can only appear at locations where the particle gradient is sharp enough.

Examining a total of 11 solar particle events observed during the *Ulysses* high-latitude passage during the 2000–2001 solar maximum (McKibben et al. 2003; Dalla et al. 2003), we found only two additional events where brief periods of large cross-field anisotropy were observed. Figure 4 shows one event in 2000 September, when *Ulysses* was at 2.8 AU and S70°. The anisotropy is directed along the magnetic field for most of the time; however, there is brief period of $\sim$5 hr on day 256 where significant deviation of the anisotropy direction from the magnetic field direction is observed. The magnetic field direction did not change much in the short 5 hr period of large cross-field anisotropy, so we are unable to determine the diffusion coefficient. Given the fact that sizeable anisotropy can only appear in a small region of the heliosphere where the density gradient is sharp enough, we consider ourselves very fortunate to observe the large diffusion anisotropy for many hours during the 2000 July 14 event.

Using the observed fact that we did not see any change in the anisotropy when the magnetic field switched its polarity around 0000 UT on day 197, we can place an upper limit for the antisymmetric term of the diffusion tensor. The $\kappa_A/\kappa_\perp$ ratio must be much less than 0.17 in order to show no signature of change in anisotropy within the error bar of the hourly averages in Figure 3. If we use longer averages, which must have smaller error bars, the upper limit of the $\kappa_A/\kappa_\perp$ ratio could be further reduced.

4. CONCLUSION AND DISCUSSION

From the above analysis of the anisotropy measurements of the 2000 July 14 event, we have derived a large $\kappa_\perp/\kappa_\parallel$ ratio of 0.25 with quite a high level of confidence. A large $\kappa_\perp/\kappa_\parallel$ ratio is also needed to explain the *Ulysses* observations of the very small latitude gradient of cosmic-ray intensity at both solar minimum and solar maximum. It is consistent with the analysis by Dwyer et al. (1997) of low-energy particles accelerated by CIRs. Now we confirm that large perpendicular diffusion also occurs in solar energetic particles. This can be used to explain the reservoir effect seen in the decay phase of large SEP events. Our observation further extends the need of consideration of perpendicular transport even in the early phase of SEP events. Although in many events we do not see cross-field particle flow directly at the location of a spacecraft, perpendicular diffusion can occur elsewhere that may affect our observations far away.

The upper limit $\kappa_A/\kappa_\perp \lll 0.17$ is also interesting. We may rewrite this, in the applicable limit $\lambda \ggg r_g$, as $\kappa_A = \nu r_g/3$. The perpendicular diffusion length must satisfy $\lambda_\perp \equiv 3\kappa_\perp/\nu \ggg 6r_g$, or $\kappa_\perp \ggg \sim 5 \times 10^{20}$ cm^2 s^{-1}, which is consistent with the value derived earlier. This is another constraint imposed by the large perpendicular diffusion.

The observed large $\kappa_\perp/\kappa_\parallel$ ratio and small $\kappa_A/\kappa_\perp$ ratio provide a tough challenge to the theory of particle transport in turbulent magnetic fields. So far, as far as we know, no theory has been able to produce a $\kappa_\perp/\kappa_\parallel$ ratio higher than 10%. Because $\kappa_A = \nu r_g/3$ is determined by the particle gyromotion, an upper limit of the $\kappa_A/\kappa_\perp < 0.17$ ratio means that particles are scattered before completing one circle or that the scattering time is shorter than the gyroperiod. Under this condition, we probably have to consider magnetic turbulence of much smaller scales than the gyroradius in the calculation of particle diffusion coefficient.

The work was partially supported by NASA grants NAG 5-10888 and NAG 5-11036 and by JPL subcontract 1240373. M. Z. thanks J. Dwyer for discussion of the method of anisotropy analysis inspired from his paper. The work of J. R. J. was supported in part by NASA under grant 10990 and by NSF under grant ATM 00-01444.

REFERENCES

Balogh, A., Beek, T. J., Forsyth, R. J., Hedgecock, P. C., Marquedant, R. J., Smith, E. J., Southwood, D. J., & Tsurutani, B. T. 1992, A&AS, 92, 221

Bieber, J. W., & Matthaeus, W. H. 1997, ApJ, 485, 655

Bieber, J. W., Matthaeus, W. H., Smith, C. W., Wanner, W., Kallenrode, M.-B., & Wibberenz, G. 1994, ApJ, 420, 294

Cane, H. V., McGuire, R. E., & von Rosenvinge, T. T. 1986, ApJ, 301, 448

Dalla, S., et al. 2003, Ann. Geophys., 21, 1367

Dwyer, J. R., Mason, G. M., Mazur, J. E., Jokipii, J. R., von Rosenvinge, T. T., & Lepping, R. P. 1997, ApJ, 490, L115

Fisk, L. A. 1996, J. Geophys. Res., 101, 15,547

Forman, M. A., & Gleeson, L. J. 1975, Ap&SS, 32, 77

Forman, M. A., Jokipii, J. R., & Owens, A. J. 1974, ApJ, 192, 535

Giacalone, J., & Jokipii, J. R. 1994, ApJ, 430, L137

———. 1999, ApJ, 520, 204

Gleeson, L. J. 1969, Planet. Space Sci., 17, 31

Intriligator, D. S., & Siscoe, G. L. 1995, J. Geophys. Res., 100, 21,605

Isenberg, P. A., & Jokipii, J. R. 1979, ApJ, 234, 746

Jokipii, J. R. 1966, ApJ, 146, 480

Jokipii, J. R., & Kota, J. 1995, Space Sci. Rev., 72, 379

Kahler, S. W., Hildner, E., & van Hollebeke, M. A. 1978, Sol. Phys., 57, 429

Kota, J., & Jokipii, J. R. 1982, Geophys. Res. Lett., 9, 656

———. 1983, ApJ, 265, 573

McKibben, R. B., Lopate, C., & Zhang, M. 2001, Space Sci. Rev., 97, 257

McKibben, R. B., et al. 2003, Ann. Geophys., 21, 1217

Ng, C. K., & Reames, D. V. 1994, ApJ, 424, 1032

Palmer, I. D. 1982, Rev. Geophys., 20, 335

Potgieter, M. S. 2000, J. Geophys., Res., 105, 18,295

Reames, D. V. 1999, Space Sci. Rev., 90, 413

Reid, G. C. 1964, J. Geophys. Res., 69, 2659

Reinecke, J. P. L., Moraal, H., & McDonald, F. B. 1993, J. Geophys. Res., 98, 9417

———. 1996, J. Geophys. Res., 101, 21,581

Roelof, E. C. 1969, in Lectures in High Energy Astrophysics, ed. H. Ogelmann & J. R. Wayland (NASA SP-199; Washington: NASA), 111

Simpson, J. A., et al. 1992, A&AS, 92, 365

Zhang, M., McKibben, R. B., Lopate, C., Jokipii, J. R., Giacalone, J., Kallenrode, M.-B., & Rassoul, H. K. 2003, J. Geophys. Res., 108, 1154

Zwickl, R. D., & Roelof, E. C. 1981, J. Geophys. Res., 86, 5449